JACS
JOURNAL OF THE AMERICAN CHEMICAL SOCIETY
Article
pubs.acs.org/JACS

Mechanism and Selectivity of *N*-Triflylphosphoramide Catalyzed ($3^+ + 2$) Cycloaddition between Hydrazones and Alkenes

Xin Hong,[†,∥] Hatice Başpınar Küçük,[‡,∥] Modhu Sudan Maji,[‡] Yun-Fang Yang,[†] Magnus Rueping,*[,‡] and K. N. Houk*[,†]

[†]Department of Chemistry and Biochemistry, University of California, Los Angeles, California 90095, United States
[‡]Institute of Organic Chemistry, RWTH Aachen University, Landoltweg 1, 52074 Aachen, Germany

Supporting Information

ABSTRACT: Brønsted acid catalyzed ($3^+ + 2$) cycloadditions between hydrazones and alkenes provide a general approach to pyrazolidines. The acidity of the Brønsted acid is crucial for the catalytic efficiency: the less acidic phosphoric acids are ineffective, while highly acidic chiral *N*-triflylphosphoramides are very efficient and can promote highly enantioselective cycloadditions. The mechanism and origins of catalytic efficiencies and selectivities of these reactions have been explored with density functional theory (M06-2X) calculations. Protonation of hydrazones by *N*-triflylphosphoramide produces hydrazonium−phosphoramide anion complexes. These ion-pair complexes are very reactive in ($3^+ + 2$) cycloadditions with alkenes, producing pyrazolidine products. Alternative 1,3-dipolar (3 + 2) cycloadditions with the analogous azomethine imines are much less favorable due to the endergonic isomerization of hydrazone to azomethine imine. With *N*-triflylphosphoramide catalyst, only a small distortion of the ion-pair complex is required to achieve its geometry in the ($3^+ + 2$) cycloaddition transition state. In contrast, the weak phosphoric acid does not protonate the hydrazone, and only a hydrogen-bonded complex is formed. Larger distortion energy is required for the hydrogen-bonded complex to achieve the "ion-pair" geometry in the cycloaddition transition state, and a significant barrier is found. On the basis of this mechanism, we have explained the origins of enantioselectivities when a chiral *N*-triflylphosphoramide catalyst is employed. We also report the experimental studies that extend the substrate scope of alkenes to ethyl vinyl ethers and thioethers.

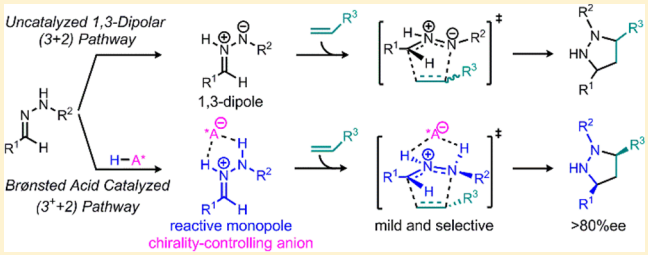

INTRODUCTION

Pyrazolidines are very important and valuable compounds for their widespread natural occurrence,[1] important biological properties,[2] and applications in material science.[3] The Lewis-acid catalyzed reactions between hydrazones and alkenes provide atom- and step-economic access to pyrazolidines,[4] and extensive effort has been devoted to the development of enantioselective catalysts for this transformation.[5,6] These reactions are found to involve formations of intermediates that undergo cycloadditions. Kobayashi discovered that chiral zirconium/BINOL complexes are efficient enantioselective Lewis acid catalysts for both inter- and intramolecular (3 + 2) cycloadditions between hydrazones and alkenes (Scheme 1a).[5a,c] In addition, Leighton and Tsogoeva individually reported that chiral silanes could serve as an alternative chiral Lewis acid for similar reactions (Scheme 1a).[5d,6c] Müller and List have also developed a chiral Brønsted-acid catalyzed asymmetric 6π electrocyclization reaction of hydrazones to obtain enantiopure pyrazolidine derivatives.[6h] Although Huisgen's definition of cycloadditions does not strictly apply to the overall reactions, we will follow common literature usage here. The Rueping laboratory recently discovered a general and highly enantioselective *N*-triflylphosphoramide catalyst for the intermolecular (3 + 2) cycloaddition between hydrazones and alkenes (Scheme 1b).[7] Several pyrazolidine derivatives were synthesized in excellent yields and enantioselectivities. A [H8]-BINOL-based *N*-triflylphosphoramide catalyst[8] was suitable for this transformation. In the process of exploring the generality of this significant cycloaddition reaction, we were interested in finding other readily available dipole acceptors. In this context, we found that the more electron-rich and hence more reactive dipole acceptor ethyl vinyl thioether is an interesting choice. We present our results on the asymmetric (3 + 2) cycloaddition reaction of hydrazones with ethyl vinyl thioether using a SPINOL-derived *N*-triflylphosphoramide catalyst[9] (Scheme 1c).

The acidity of Brønsted acid catalysts is crucial to induce reactions between hydrazones and alkenes. Less acidic phosphoric acids (pK_a = 13−14 in acetonitrile) give low yields of product irrespective of the reaction conditions, while the more acidic *N*-triflylphosphoramides[8] (pK_a = 6−7 in acetonitrile) are much more reactive catalysts, with good to excellent enantioselectivities.[7,10] Because of the necessity to use highly acidic Brønsted acid catalysts, we surmise that phosphoramides may not play a role like the classical Lewis

Received: July 2, 2014
Published: September 2, 2014

ACS Publications © 2014 American Chemical Society

dx.doi.org/10.1021/ja506660c | J. Am. Chem. Soc. 2014, 136, 13769−13780

Scheme 1. Lewis Acid and Brønsted Acid Facilitated Enantioselective (3 + 2) Cycloadditions between Hydrazones and Alkenes[a]

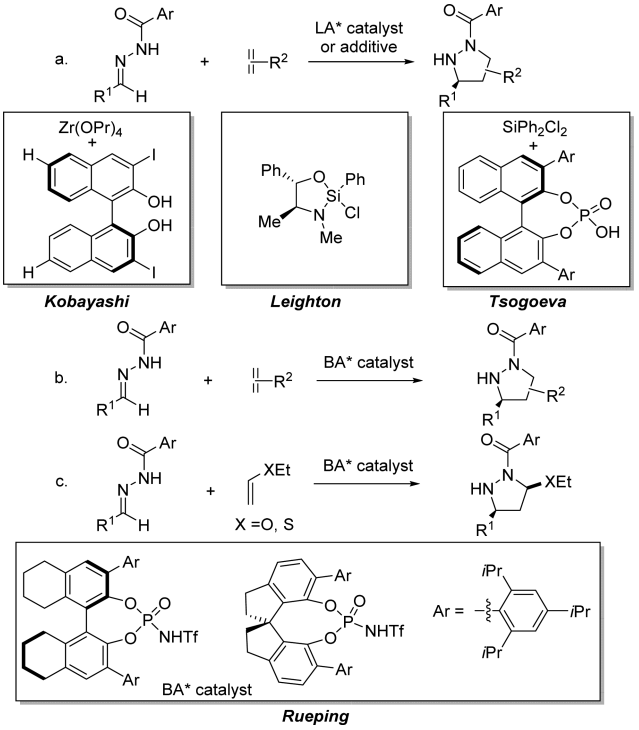

[a]LA, Lewis acid; BA, Brønsted acid.

acid catalysts in activating the 1,3-dipole.[5e,11] Instead, the Brønsted acid catalyst could protonate hydrazone and form an ion-pair complex **A**, as shown in Scheme 2. The ion-pair complex **A** has a reactive monopolar hydrazonium and a chirality-controlling phosphoramide anion. We use the word "monopole" to describe the cationic intermediate, to contrast to the variable 1,3-dipoles, neutral species bearing plus and minus charges, in favorable Lewis structures. The reaction of the monopole with alkenes or alkynes is referred to as a 1,3-monopolar cycloaddition. The $(3^+ + 2)$ cycloaddition of the ion-pair complex **A** is mild and selective via **TSB**, generating the pyrazolidine−phosphoramide complex **C**. Subsequently, complex **C** releases the pyrazolidine product, regenerating the complex **A** with another molecule of hydrazone. Although monopolar $(3^+ + 2)$ cycloadditions with hydrazonium cations have been documented since the 1970s, the synthetic applications and especially the catalytic reactions are rare.[12] Does the *N*-triflylphosphoramide really protonate hydrazones and enable the $(3^+ + 2)$ cycloadditions with alkenes? How does the chiral phosphoramide control the regio- and enantioselectivity? In order to answer the above questions and provide the mechanistic basis for designing future Brønsted acid catalyzed $(3^+ + 2)$ cycloadditions with hydrazones, we have carried out density functional theory (DFT) calculations to explore the mechanism and selectivity of the *N*-triflylphosphoramide catalyzed (3 + 2) cycloadditions between hydrazones and alkenes.

Scheme 2. Proposed Monopolar $(3^+ + 2)$ Pathway of Brønsted Acid Catalyzed Cycloaddition between Hydrazones and Alkenes

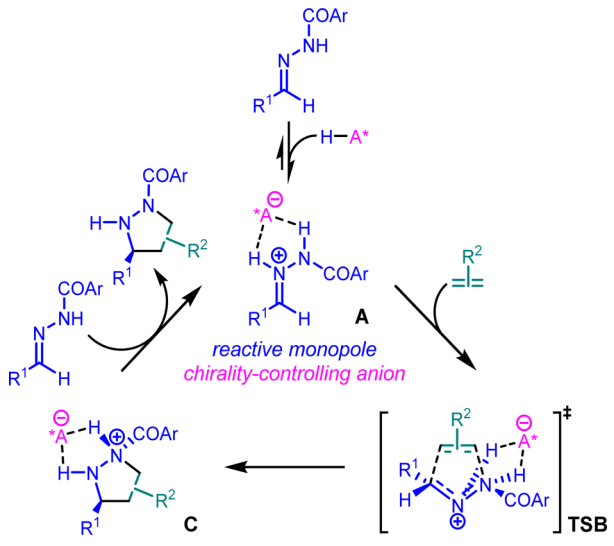

RESULTS AND DISCUSSION

Experimental Results. We started our investigation by using 1.0 equiv of hydrazone and 3.0 equiv of vinyl ethyl thioether and applying our previously reported best catalyst.[5a] First, the effect of the hydrazone protecting group on the outcome of the reaction was studied (Table 1, entries 1−3). In this regard, hydrazone **3a** with a simple benzoyl protecting group was suitable for this reaction, and cycloadduct **8a** was isolated along with its minor diastereomer in 41% yield and 40% ee (Table 1, entry 3). After intensive screening of different aromatic, oxygenated, and chlorinated solvents, 1,2-dichloroethane (DCE) was found to be the best solvent for this transformation (Table 1, entry 4). Screening of various BINOL- and [H8]-BINOL-based *N*-triflylphosphoramides and phosphoric acids did not improve these results, and we turned our attention to discover a more effective catalyst. SPINOL-derived *N*-triflylphosphoramides have not been reported so far in any asymmetric transformation.[9] In the reaction studied here, the enantioselectivity of the reaction increased to 84% ee with the new SPINOL-derived catalyst **5c** (Table 1, entry 5).[13] The enantioselectivity and yield were both further improved by lowering the reaction temperature to 0 °C (91% ee, 48%, Table 1, entry 6). The yield of the reaction could be improved further by increasing the concentration or by using 7.0 equiv of vinyl ethyl thioether (Table 1, entries 7 and 8). Finally, 3.0 equiv of the parent aldehyde employed for the hydrazone preparation as an additive was beneficial for the yield without affecting the enantioselectivity (Table 1, entry 9). Under these optimized conditions (Table 1, entry 9), hydrazone **1a** also reacted smoothly to provide the pyrazolidine derivative **6a** with excellent results (92% ee vs 25% ee, Table 1, entry 10 vs entry 1). The diastereoselectivity of the reaction was found to be 7:1, which is significantly better than the previously reported one (up to 3:1).[5c]

We next evaluated the scope of the reaction. Several hydrazones were prepared from the corresponding aldehydes and reacted under our standard reaction conditions. In general, the reactions worked with high diastereoselectivities and the major syn diastereomer was isolated along with its minor anti diastereomer (Table 2). Hydrazones **3a−e** derived from saturated long chain and branched aldehydes reacted smoothly to provide cycloadducts **8a−e** in good yields, with high diastereoselectivities and excellent enantioselectivities (50−

dx.doi.org/10.1021/ja506660c | J. Am. Chem. Soc. 2014, 136, 13769−13780

Table 1. Optimization of the Reaction Conditions for the [3 + 2] Cycloaddition Reaction with Ethyl Vinyl Thioether[a]

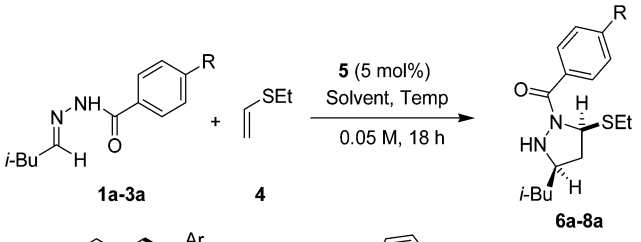

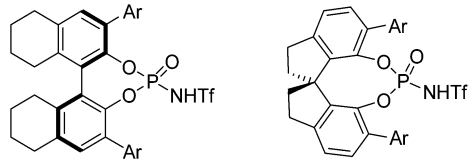

5a: Ar = TRIP
5b: Ar = 1-Naphthyl
5c: Ar = TRIP

entry	R, 1–3	BA*	solvent	temp (°C)	product 6–8	yield (%)[b]	ee (%)[c]
1	NO_2, **1a**	**5a**	$CHCl_3$	rt	**6a**	42	25
2	CF_3, **2a**	**5a**	$CHCl_3$	rt	**7a**	40	11
3	H, **3a**	**5a**	$CHCl_3$	rt	**8a**	41	40
4	H, **3a**	**5a**	DCE	rt	**8a**	55	63
5	H, **3a**	**5c**	DCE	rt	**8a**	34	84
6[d]	H, **3a**	**5c**	DCE	0	**8a**	48	91
7[d,e]	H, **3a**	**5c**	DCE	0	**8a**	55	90
8[d,f]	H, **3a**	**5c**	DCE	0	**8a**	68	87
9[d,g]	H, **3a**	**5c**	DCE	0	**8a**	75	91
10[d,g]	NO_2, **1a**	**5c**	DCE	0	**6a**	65	92

[a]Unless otherwise noted, the reactions were carried out for 18 h using 5 mol % of catalyst and 3.0 equiv of vinyl ethyl thioether in a 0.05 M solution of hydrazone with the solvent and the temperature as indicated in the table. **6a**, R = NO_2; **7a**, R = CF_3; **8a**, R = H. [b]The *syn* product was isolated along with its *anti* diastereomer in a 3:1 (at rt) to 7:1 (at 0 °C) ratio as determined by ^{1}H NMR analysis. [c]The enantioselectivity was determined by chiral HPLC analysis. [d]Reaction was performed for 4 days. [e]Reaction was conducted in 0.1 M hydrazone concentration. [f]Vinyl ethyl thioether (7.0 equiv) was used. [g]Isovaleraldehyde (3.0 equiv) was used as additive.

75%, 87–92% ee, Table 2). Hydrazones **3f,g** with heteroatoms in the long chain were also suitable substrates, and products **8f,g** were isolated with excellent enantioselectivities (43–62%, 88–90% ee). Hydrazone **3h** with a methyl ester moiety in the alkyl chain provided product **8h** with good results (42%, 83% ee). Several hydrazones **3i–k** with a C–C double bond in the alkyl chain reacted smoothly, and cycloadducts **8i–k** were isolated with excellent results (42–60%, 85–92% ee). Hydrazone **3l** with an alkyne moiety also reacted smoothly to provide adduct **8l**. More functionalized thioethers do not give the desired yields or enantioselectivities as good as observed with ethyl vinyl thioether.[14]

We also investigated the more reactive vinyl ether substrates. After some initial optimizations, we found that [H8]-BINOL-derived *N*-triflylphosphoramide catalyst **5b** is suitable for the reaction (Scheme 3). The reactions were conducted in THF as solvent, and the best results were obtained at −10 °C using 10 mol % catalyst loading. The aldehyde (3.0 equiv) used for the hydrazone preparation was found to be an important additive to obtain a good yield for the cycloaddition reaction. The reaction tolerates various alkyl substituents on vinyl ethers with

Table 2. Substrate Scope of the Organocatalytic Enantioselective [3 + 2] Cycloaddition Reaction with Vinyl Ethyl Thioether[a]

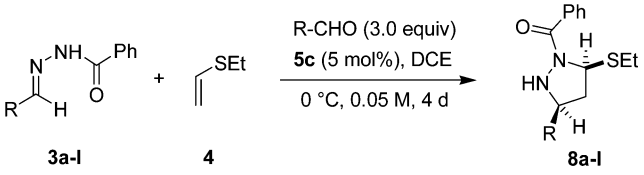

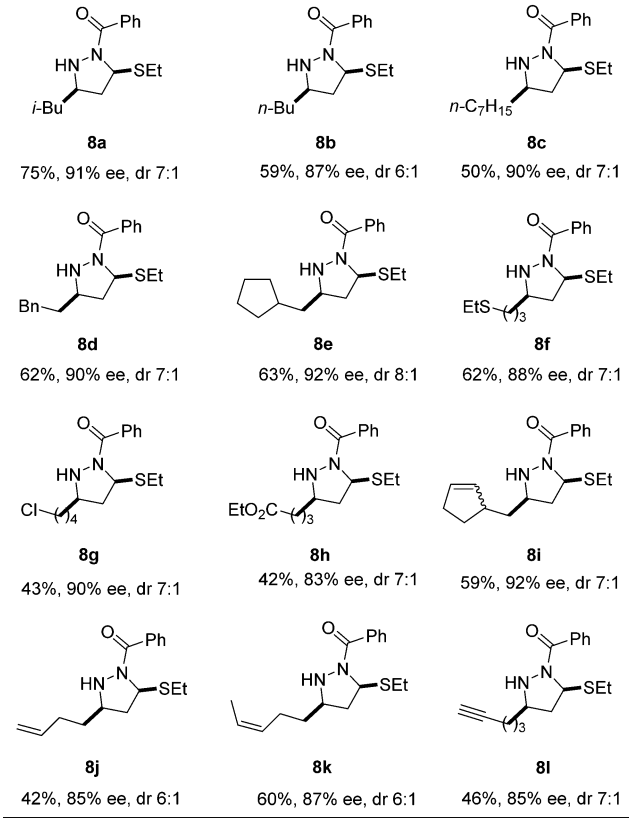

[a]Diastereomeric ratio was determined by ^{1}H NMR analysis. Enantiomeric excesses were determined by HPLC analysis.

Scheme 3. Organocatalytic Enantioselective [3 + 2] Cycloaddition Reaction with Ethyl Vinyl Ether[a]

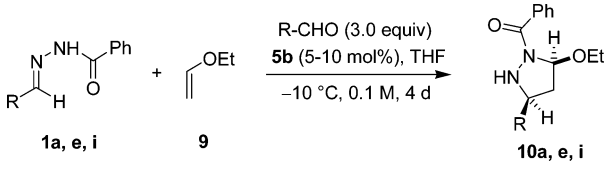

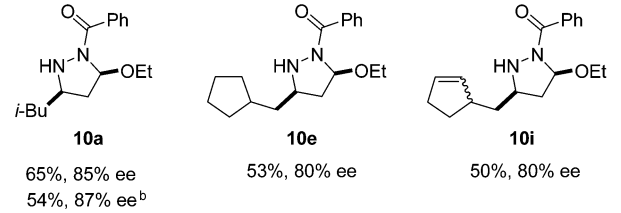

[a]Greater than 95:5 dr (the second diastereomer was not observed in the ^{1}H NMR analysis). Enantiomeric excesses were determined by HPLC analysis. [b]The reaction was conducted by using 5 mol % catalyst loading.

dx.doi.org/10.1021/ja506660c | J. Am. Chem. Soc. 2014, 136, 13769–13780

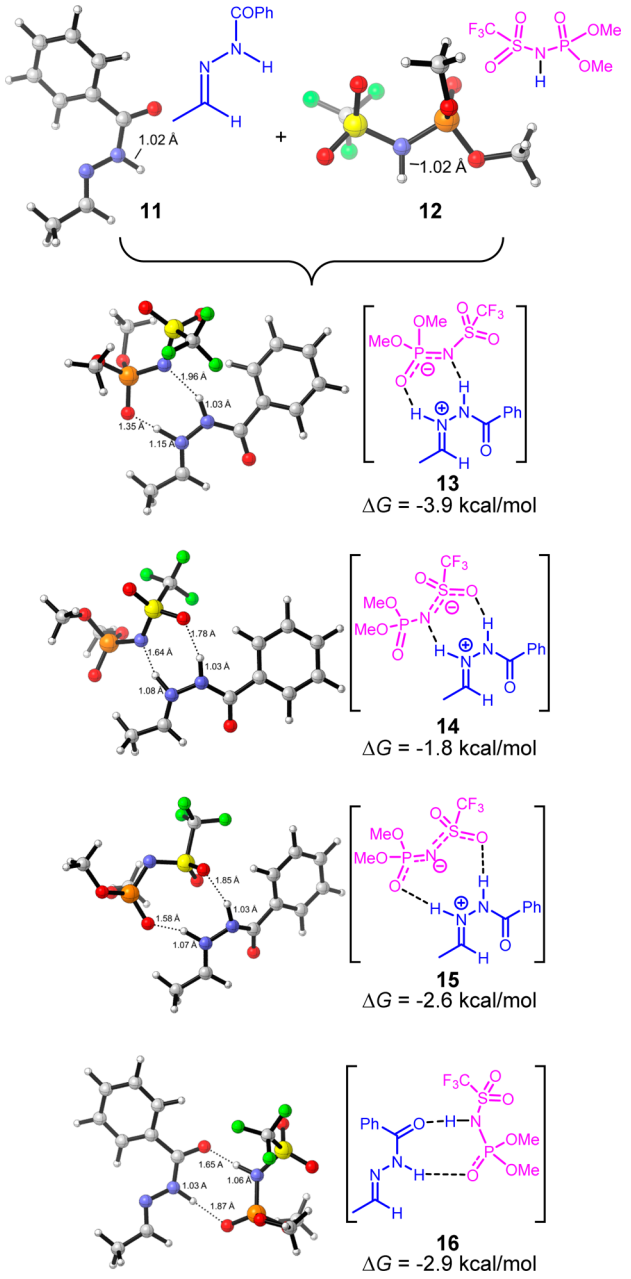

Figure 1. Optimized structures and Gibbs free energies of complexes between hydrazone **11** and phosphoramide **12**.

good to high enantioselectivities, and the ethyl vinyl ether gives the highest yield.[15] This cycloaddition reaction can also be performed with different aliphatic aldehyde derived hydrazones with good yields and high enantioselectivities (50−65%, 80−85% ee, Scheme 3). Decreasing the catalyst loading to 5 mol % afforded cycloadduct **10a** in 54% yield and 87% ee under similar conditions. Further attempts with enamides only give racemic products or no desired cycloadducts.[16]

Computational Results. *Computational Methods.* All DFT calculations were performed with Gaussian 09.[17] Geometry optimization was carried out with the M06-2X[18] level of theory and the 6-31G(d) basis set. The vibrational frequencies were computed at the same level to check whether each optimized structure is an energy minimum or a transition state and to evaluate its zero-point vibrational energy (ZPVE) and thermal corrections at 298 K. The single-point energies and solvent effects in chloroform were computed with M06-2X method and the 6-311+G(d,p) basis set, based on the gas-phase optimized structures. Solvation energies were evaluated by a self-consistent reaction field (SCRF) using the CPCM model[19] (UFF radii). Fragment distortion and interaction energies and bond dissociation energies were computed at the M06-2X/6-311+G(d,p) level using the M06-2X/6-31G(d) geometries in the gas phase. Extensive conformational searches for the hydrazone, phosphoramide, and hydrazone−phosphoramide/phosphate complexes have been conducted, and only the most stable conformers and isomers are discussed.

Complexation between Hydrazone and Phosphoramide. We explored first the nature of complexes formed between the model hydrazone **11** and the achiral model phosphoramide **12**. The optimized structures and Gibbs free energies of these complexes are shown in Figure 1.[20] The complexation between hydrazone and phosphoramide can occur with or without proton transfer. When proton transfer occurs, there are three possible hydrogen-bonding complexes; these complexes (**13**, **14**, and **15**) are shown in Figure 1. The N−H distances of hydrazonium in the ion-pair complexes are generally smaller than 1.1 Å, and the distances between phosphoramide anion and hydrogens from hydrazonium are at least 1.6 Å. The proton transfer complexes support the hypothesis that the Brønsted acid facilitates the $(3^+ + 2)$ cycloaddition by generating the hydrazonium cation. Alternatively, only hydrogen-bonding complexation occurs in complex **16**.[21] The N−H distances are similar to those of the separate hydrazone and phosphoramide. Although the ion-pair and hydrogen-bonded complexes are quite different, the complexation reactions are all exergonic, and the four complexes have similar stabilities, 2 to 4 kcal/mol more stable than separate reactants.

(3 + 2) Cycloaddition with Hydrazone−Phosphoramide Complex. The (3 + 2) cycloaddition between the hydrazone−phosphoramide complexes and ethylene was explored, and the optimized structures and Gibbs free energies of transition states (compared with the most stable complex **13**) are shown in Figure 2. **TS17**, **TS18**, and **TS19** are the transition states with the ion-pair complexes (**13**, **14**, and **15**), and **TS20** is the transition state with the hydrogen-bonded complex **16**. The ion-pair complexes are much more reactive than the hydrogen-bonded complex in the (3 + 2) cycloaddition with ethylene. The reaction barriers of the ion-pair complexes (**TS17**, **TS18**, and **TS19**) are around 30 kcal/mol, while the hydrogen-bonded complex has a significantly higher barrier via **TS20** (51.3 kcal/mol).[22] Only the ion-pair complexes are reactive in the (3 + 2) cycloaddition with alkenes, and the ion-pair complexes have similar reactivities to the hydrazonium cation that we investigated earlier.[23] The *N*-triflylphosphoramide catalyzed cycloaddition between hydrazones and alkenes is, indeed, a $(3^+ + 2)$ cycloaddition. Among the transition states with the ion-pair complexes, **TS19** is the most favorable one with a barrier of 28.6 kcal/mol, while **TS17** and **TS18** are at least 2 kcal/mol higher in terms of Gibbs free energy. This suggests that the phosphoramide anion uses the two terminal oxygens (one adjacent to phosphine, the other adjacent to sulfur) to bind the hydrazonium cation in the $(3^+ + 2)$ cycloaddition transition state.

Monopolar $(3^+ + 2)$ vs Dipolar (3 + 2) Cycloadditions. We also studied the whole catalytic cycle of the $(3^+ + 2)$ cycloaddition and the competing 1,3-dipolar (3 + 2) cycloaddition pathway with the model hydrazone **11** and phosphoramide **12** (Figure 3). From hydrazone **11**, the complexation with phosphoramide **12** is exergonic by 3.9 kcal/mol, giving the ion-pair complex **13**. Subsequent $(3^+ + 2)$ cycloaddition with ethylene requires a barrier of 28.6 kcal/mol via **TS19**, giving the pyrazolidine−phosphoramide complex **21**. The pyrazolidine product **22** is less basic than the hydrazone **11**, so the product extrusion from complex **21** to regenerate the ion-pair complex **13** is exergonic, making the overall reaction exergonic by 11.0 kcal/mol. The ion-pair complex **13** is the resting state of the whole catalytic cycle, and the overall barrier is 28.6 kcal/mol via transition state **TS19**.[25] Alternatively, the hydrazone can isomerize to the less stable azomethine imine **23** and undergo the 1,3-dipolar (3 + 2) cycloaddition with ethylene. Although the azomethine imine is a reactive dipole and the cycloaddition barrier with ethylene is only 26.8 kcal/mol, the overall barrier of the 1,3-dipolar cycloaddition pathway is 38.5 kcal/mol because of endergonic isomerization. Therefore, the

dx.doi.org/10.1021/ja506660c | J. Am. Chem. Soc. 2014, 136, 13769−13780

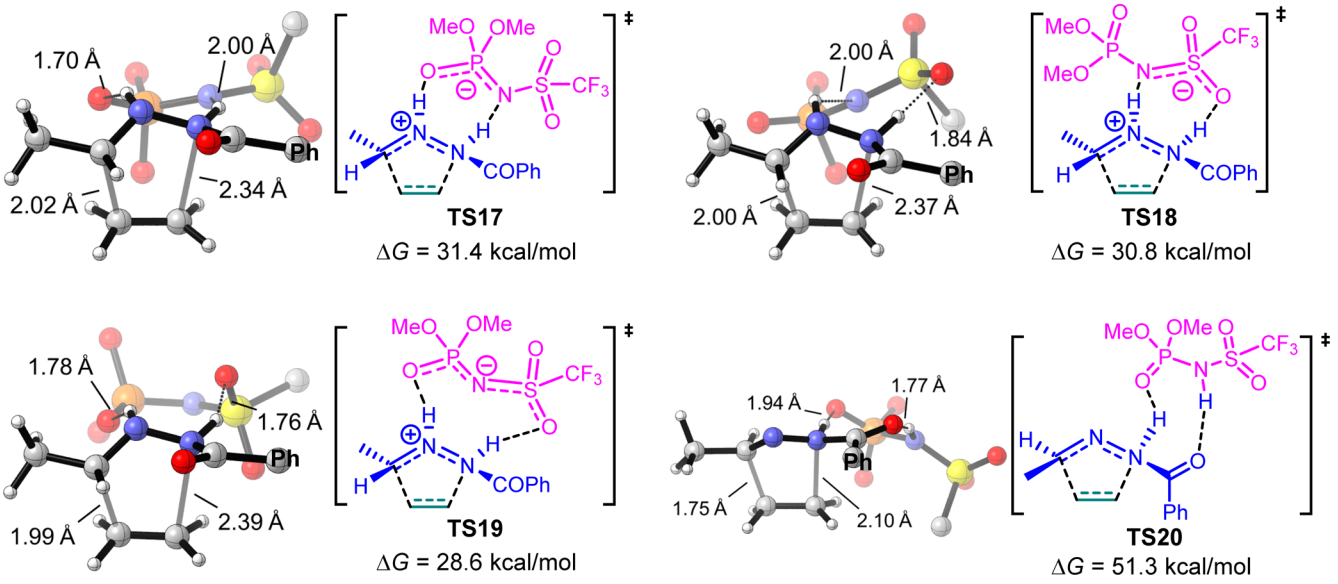

Figure 2. Optimized structures and Gibbs free energies of (3 + 2) cycloaddition transition states between the hydrazone–phosphoramide complexes and ethylenes (the free energies changes are compared with the most stable complex **13**; the phenyl group from hydrazone and the methyl groups and fluorines from phosphoramide are hidden for simplicity).[24]

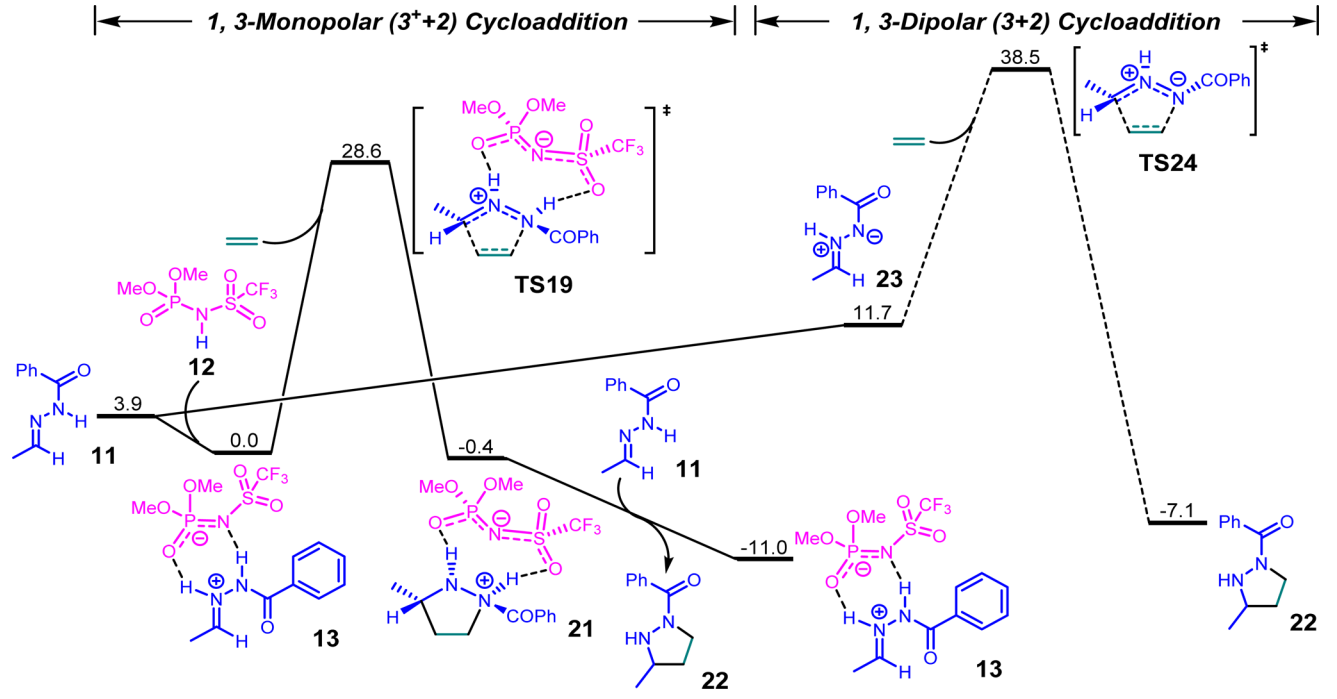

Figure 3. Free energy profile of the phosphoramide **12** catalyzed 1,3-monopolar (3^+ + 2) cycloaddition pathway and the 1,3-dipolar (3 + 2) cycloaddition pathway between hydrazone **11** and ethylene. Gibbs free energies are shown in kcal/mol.

phosphoramide catalyzed (3^+ + 2) cycloaddition pathway is much more favorable than the 1,3-dipolar cycloaddition pathway.

Catalytic Activities of Phosphoramide and Phosphoric Acid. Recent experiments have shown that the *N*-triflylphosphoramide is a much more effective catalyst than phosphoric acid for the cycloaddition between hydrazones and alkenes. We have used DFT calculations to explain the different catalytic activities of the two Brønsted acids, and the results are shown in Figure 4. As described above, the *N*-triflylphosphoramide catalyzed (3 + 2) cycloaddition between hydrazone **11** and ethylene requires a 28.6 kcal/mol barrier via **TS19**. In contrast, the same reaction catalyzed by the less acidic phosphoric acid, modeled by the dimethyl phosphate **25**, is much more difficult. From the hydrazone **11**, the complexation with phosphate is exergonic by 4.4 kcal/mol, generating the hydrazone–phosphate complex **26**. The subsequent (3 + 2) cycloaddition with ethylene via **TS27** requires a barrier of 36.8 kcal/mol, which is substantially higher than the barrier of the *N*-triflylphosphoramide catalyzed pathway.

In order to understand the different catalytic efficiencies of phosphoric acid and *N*-triflylphosphoramide, we applied the distortion/interaction model[26−28] on the cycloaddition transition states (**TS19** and **TS27**). Both transition states were separated into two fragments (the distorted complex and ethylene), followed by single point energy calculations on each distorted fragment. The energy differences between the distorted structures and optimized ground state structures are the distortion energies of the ion pair

dx.doi.org/10.1021/ja506660c | J. Am. Chem. Soc. 2014, 136, 13769−13780

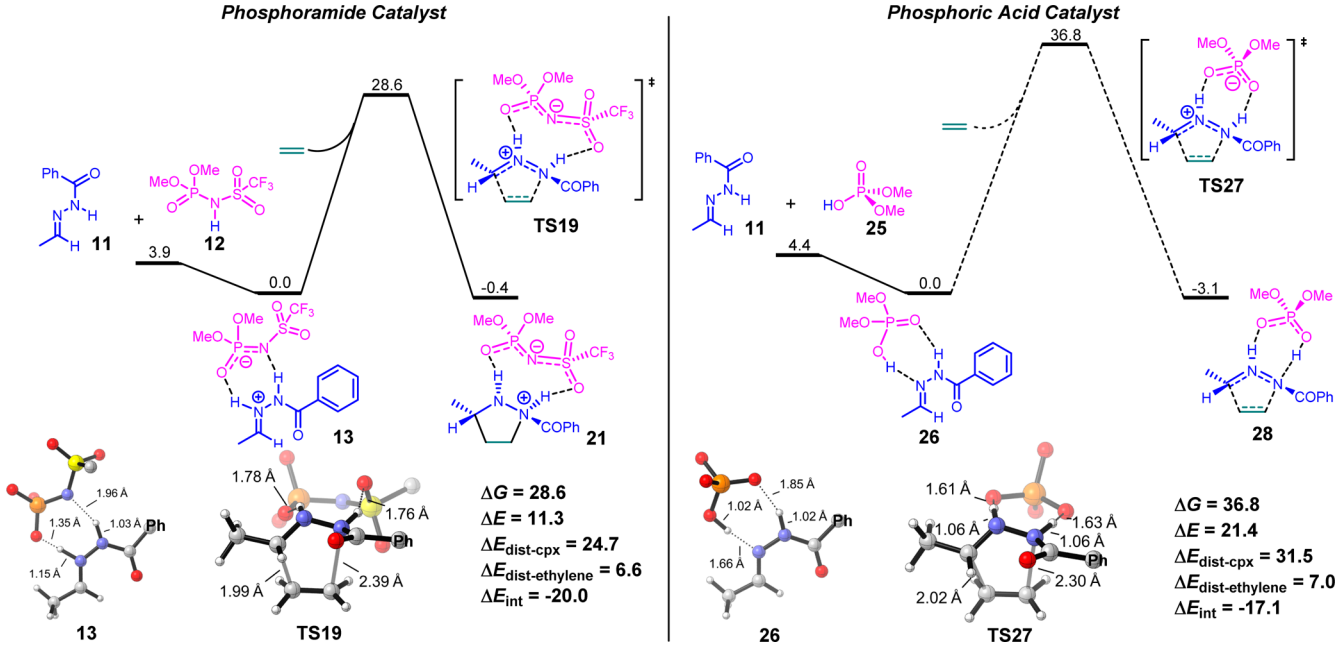

Figure 4. Free energy changes and distortion/interaction analysis of phosphoramide (**12**) and phosphoric acid (**25**) catalyzed (3 + 2) cycloadditions between hydrazone **11** and ethylene (the phenyl group from **11**, the methyl groups and fluorines from **12**, and the methyl groups from **25** are hidden for simplicity).

Scheme 4. Experimental Results and Computational Models of Selectivities of Chiral Phosphoramide 5a Catalyzed Cycloaddition between Hydrazone 29 and α-Methylstyrene 30

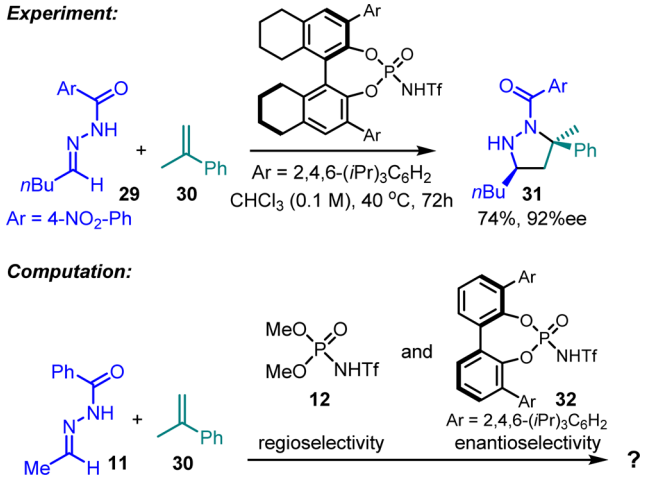

complex ($\Delta E_{\text{dist-cpx}}$) and ethylene ($\Delta E_{\text{dist-ethylene}}$), respectively. The interaction energy (ΔE_{int}) is the difference between the activation energy and the total distortion energy ($\Delta E_{\text{dist-cpx}} + \Delta E_{\text{dist-ethylene}}$).

We find that the distortion of complex ($\Delta E_{\text{dist-cpx}}$) is the determining factor for the barrier differences. Both transition states have similar $\Delta E_{\text{dist-ethylene}}$ and ΔE_{int}, while the $\Delta E_{\text{dist-cpx}}$ of phosphoric acid (31.5 kcal/mol) is 6.8 kcal/mol higher than that of phosphoramide (24.7 kcal/mol). The difference of $\Delta E_{\text{dist-cpx}}$ is the major contribution to the 10.1 kcal/mol difference of the electronic barriers (11.3 kcal/mol of **TS19** and 21.4 kcal/mol of **TS27**). The high $\Delta E_{\text{dist-cpx}}$ with dimethylphosphate means that the ground state structure of the phosphoric acid complex is very different from its structure in the transition state (**TS27**), and a large energy penalty is required for that structural change. The large structural difference arises from the low acidity of phosphoric acid. In the hydrazone–dimethylphosphate complex **26**, the hydrazone is not protonated, and the O–H bond of dimethylphosphate is 1.02 Å. Thus, the complex **26** is a hydrogen-bonded complex instead of an ion-pair complex. While in **TS27**, in order to undergo the facile (3^+ + 2) cycloaddition, the complex is distorted to an "ion pair" structure and the same O–H bond of dimethylphosphate is stretched to 1.61 Å (Figure 4). Therefore, significant distortion is required for the hydrazone–phosphoric acid complex to achieve its structure in the (3^+ + 2) cycloaddition transition state with alkenes.

Different from the phosphoric acid, *N*-triflylphosphoramide is acidic enough to protonate the hydrazone. Spontaneously, it requires much

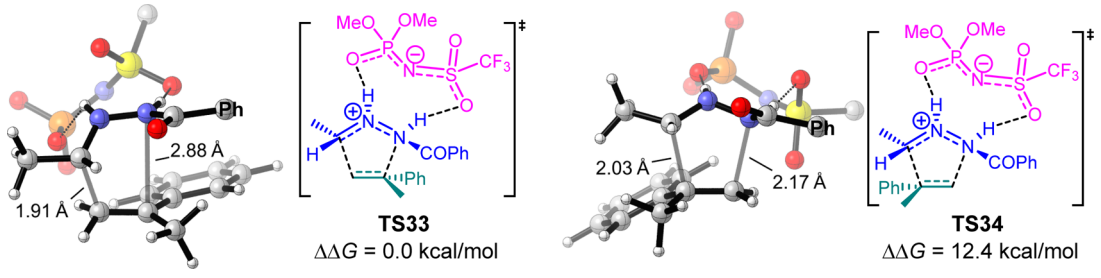

Figure 5. Transition states and relative Gibbs free energies of phosphoramide **12** catalyzed cycloaddition between hydrazone **11** and α-methylstyrene.

dx.doi.org/10.1021/ja506660c | J. Am. Chem. Soc. 2014, 136, 13769–13780

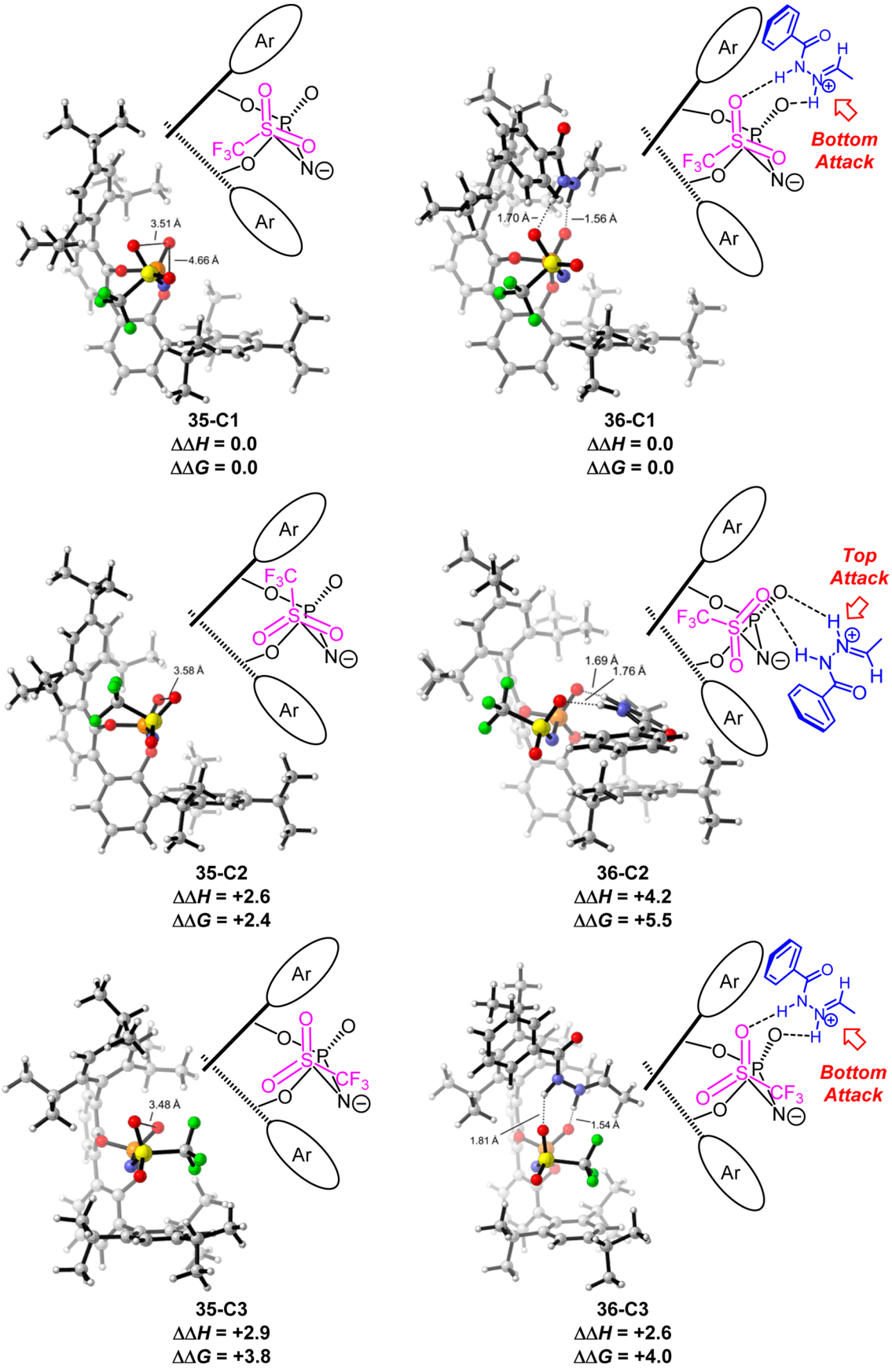

Figure 6. Optimized structures and relative stabilities of chiral *N*-triflylphosphoramide **32** anion and anion−hydrazonium complex.

dx.doi.org/10.1021/ja506660c | *J. Am. Chem. Soc.* 2014, 136, 13769−13780

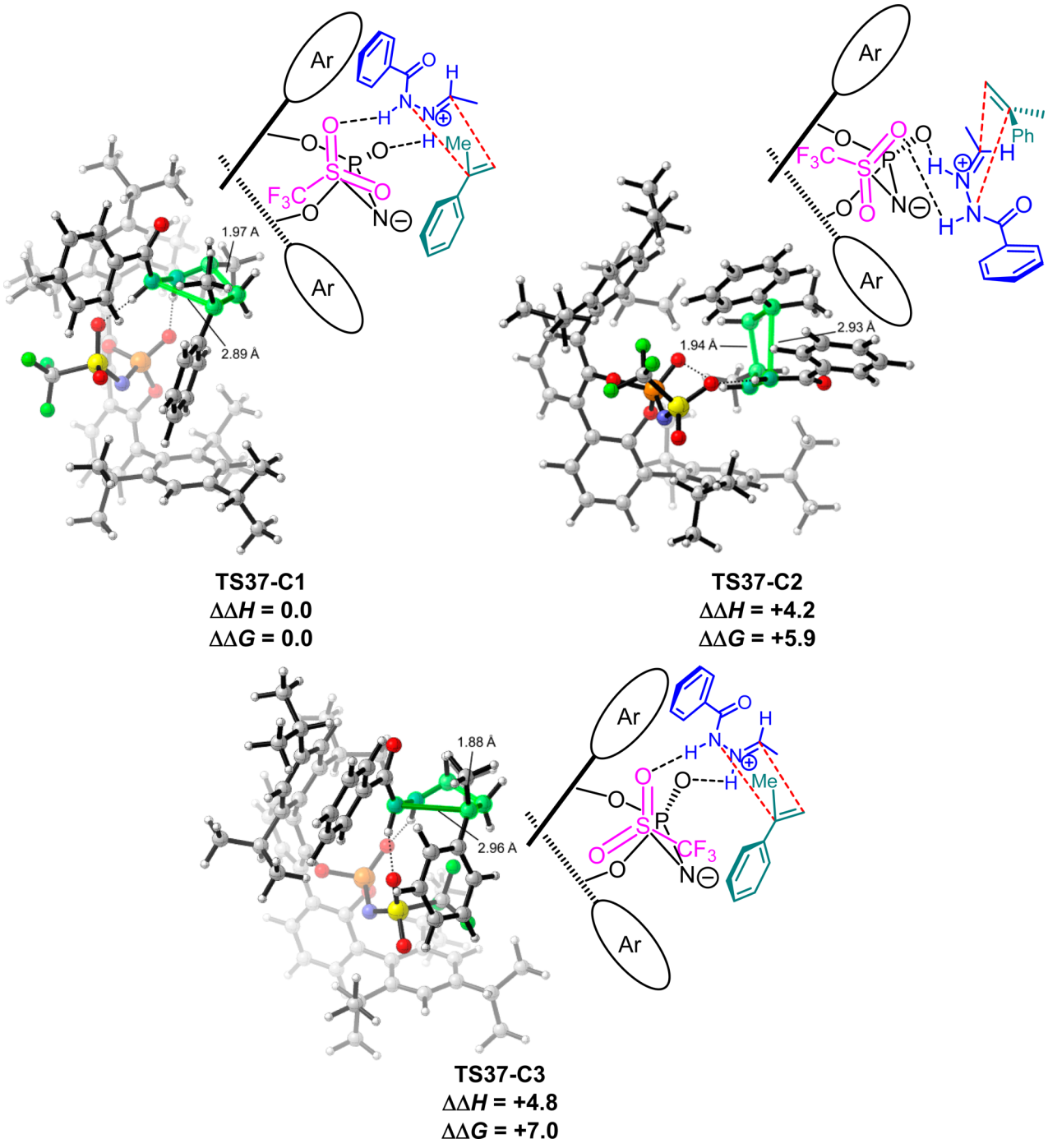

Figure 7. Optimized structures and relative stabilities of chiral *N*-triflylphosphoramide **32** catalyzed (3 + 2) cycloaddition transition states between hydrazone and α-methylstyrene.

less energy to distort the ion-pair complex **13** to the similar geometry in the transition state **TS19**, and a smaller barrier is found. In addition, to directly compare the acidity of the model phosphoric acid and *N*-triflylphosphoramide, we also calculated the free energy change of proton transfer from the *N*-triflylphosphoramide **12** to dimethylphosphate anion. The reaction is exergonic by 11.7 kcal/mol, which is consistent with the difference of $\Delta E_{\text{dist-cpx}}$ as well as the experimental pK_a difference of similar compounds measured by Rueping and coworkers.[10]

Regio- and Enantioselectivity. Because all three experimental chiral phosphoramides (**5a**, **5b**, and **5c**) bear similar chiral skeletons and prefer the same enantiomer product, we chose to study the chiral *N*-triflylphosphoramide **5a**. This catalyst gives high regio- and enantioselectivity of the cycloaddition between hydrazones and styrenes experimentally. The achiral phosphoramide **12** was used to explore the regioselectivity, and the chiral phosphoramide **32** was employed for the computations of enantioselectivity (Scheme 4).

With the model phosphoramide **12**, we have studied the regioselectivity of cycloaddition between hydrazone **11** and α-methylstyrene **30** (Figure 5). **TS33** has the phenyl group of α-methylstyrene proximal to the forming C–N bond, generating the product that has been found in experiment.[20] Computationally, we also found that **TS33** is 12.4 kcal/mol more stable than **TS34**. The regioselectivity mainly arises from the different orbital interactions between the hydrazonium and alkene in the transition states. The hydrazonium is electrophilic, and styrene is nucleophilic; thus stronger

dx.doi.org/10.1021/ja506660c | J. Am. Chem. Soc. 2014, 136, 13769–13780

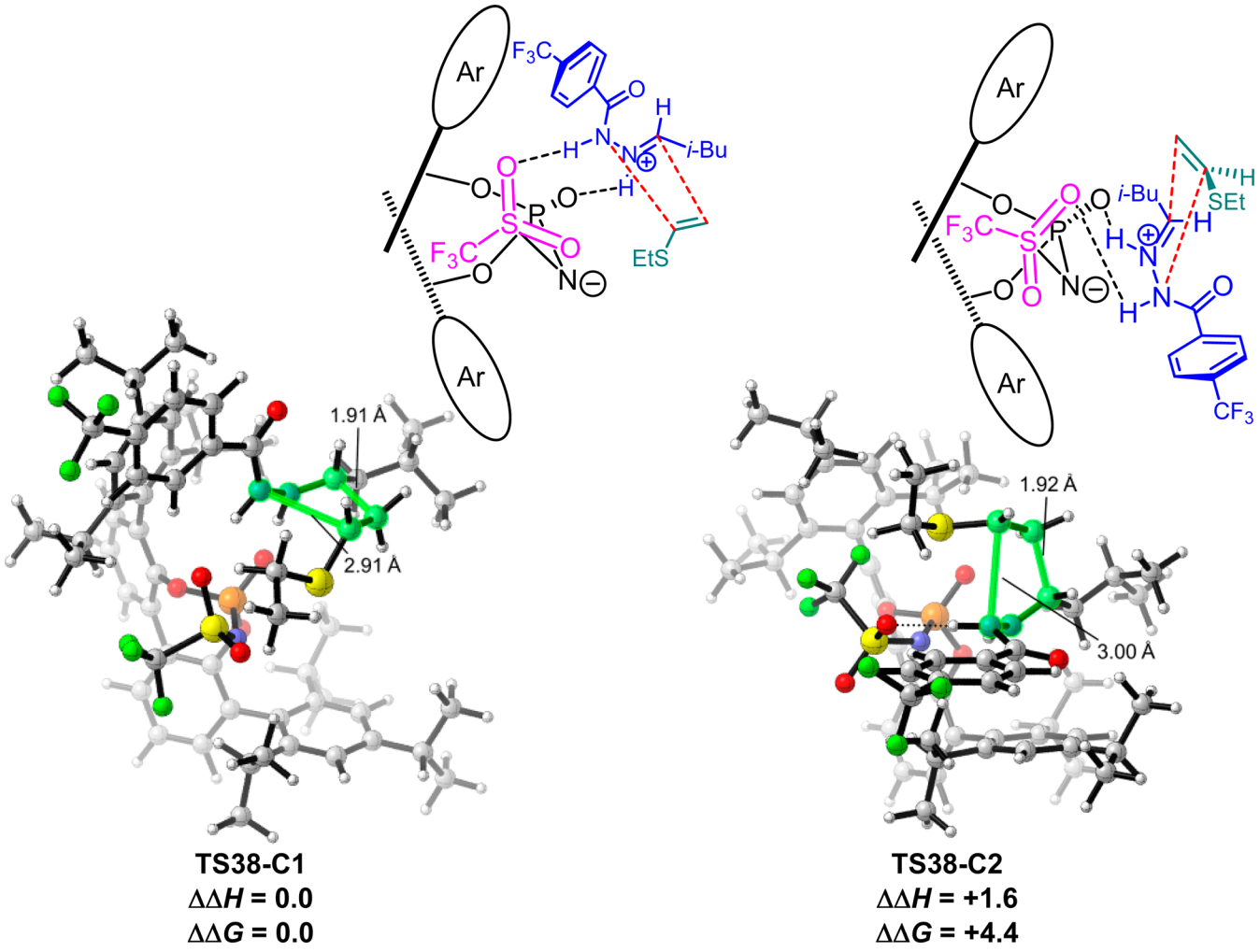

Figure 8. Optimized structures and relative stabilities of chiral *N*-triflylphosphoramide **32** catalyzed (3 + 2) cycloaddition transition states between hydrazone **2a** and ethyl vinyl thioether.

interaction can be generated when the more electrophilic terminus (carbon) of hydrazonium is proximal to the more nucleophilic terminus (terminal carbon) of styrene. This frontier molecular orbital (FMO) control leads to the strong regioselectivity.

We also studied the enantioselectivity of (3 + 2) cycloaddition between hydrazone **11** and α-methylstyrene **30** with the model chiral *N*-triflylphosphoramide **32** (Scheme 4).[29] Anion **35** has three major conformations by rotating the substituents of sulfur (Figure 6). The **35-C1** has the CF_3 group pointing away from the two bulky 2,4,6-$(iPr)_3C_6H_2$ substituents, and this conformer is the most stable. The other two conformers (**35-C2** and **35-C3**) have the CF_3 group closer to the bulky aryl substituents and are higher in energy.

As discussed above, we showed that the phosphoramide anion uses the two terminal oxygens to bind the hydrazonium in the (3 + 2) cycloaddition transition state with alkenes. Using the same binding mode, we studied the ion-pair complexes with the three conformers of **35** (Figure 6). From **35-C1**, only one pair of oxygens (with the distance of 3.51 Å) is able to form a stable complex with hydrazonium because of the distance between the oxygens, and the formed complex is **36-C1**. Similarly, **36-C2** and **36-C3** are found with the corresponding conformers of **35**. Interestingly, all three conformers of the ion-pair complex (**36-C1** to **36-C3**) have only one face available for alkenes to approach. Complex **36-C1** has the top of the hydrazonium protected by the bulky aryl substituent; the alkene can only approach from the bottom. Complex **36-C3** also has the bottom face available; thus **36-C1** and **36-C3** give the same cycloaddition product. Alternatively, **36-C2** has the bottom of the hydrazonium hindered, and this conformer leads to the minor enantiomer in experiment. Because the binding between hydrazonium and phosphoramide anion is very similar in the three conformers, **36-C1** is the most stable.

The (3 + 2) cycloaddition transition states between the three conformers of ion-pair complex and α-methylstyrene were located. The computational selectivity is consistent with the experimental results (Figure 7). We find **TS37-C1** is more favorable than **TS37-C2**, and the preference is similar to the relative stabilities of the corresponding conformers of ion-pair complex (**36**) and phosphoramide anion (**35**). Therefore, the two bulky aryl substituents of the chiral *N*-triflylphosphoramide differentiate the stabilities of the anion conformers, and the ion-pair complexation with hydrazonium transfers the chirality of the catalyst to the cycloaddition transition state, generating the enantioselectivity.

We also computationally examined the low enantioselectivity of ethyl vinyl thioether with the same chiral phosphoramide catalyst **32**. The optimized structures of cycloaddition transition states (**TS38-C1** and **TS38-C2**) and their relative stabilities are shown in Figure 8. The calculated enantioselectivity ($\Delta\Delta H$ = 1.6 kcal/mol and $\Delta\Delta G$ = 4.4 kcal/mol, Figure 8) is much lower compared with that of α-methylstyrene ($\Delta\Delta H$ = 4.2 kcal/mol and $\Delta\Delta G$ = 5.9 kcal/mol, Figure 8), which is in agreement with the experiments. This low enantioselectivity is because the thioethers are more reactive and less sterically demanding, and thus the large binding pocket of the [H8]-BINOL-based *N*-triflylphosphoramide catalyst does not provide the same high enantioselectivity as the cases with α-methylstyrene. The SPINOL-based *N*-triflylphosphoramide catalyst has a more rigid

dx.doi.org/10.1021/ja506660c | J. Am. Chem. Soc. 2014, 136, 13769−13780

backbone and a smaller binding pocket and gives high enantioselectivities even with the more reactive thioethers.[30]

CONCLUSIONS

We have developed a chiral Brønsted acid catalyzed highly asymmetric (3 + 2) cycloaddition reaction of hydrazones with ethyl vinyl thioether. The reaction can be performed with a broad range of aliphatic aldehyde hydrazones to give valuable pyrazolidine derivatives in good yields, with high diastereoselectivities and excellent enantioselectivities. Our results clearly indicated that SPINOL-derived *N*-triflylphosphoramide catalysts can also be a good choice for asymmetric Brønsted acid catalysis, especially when the corresponding BINOL-derived catalysts fail to provide good results. The cycloaddition reaction was also performed with ethyl vinyl ether, and the corresponding pyrazolidine derivatives were synthesized with high enantioselectivities. The mechanism and origins of catalytic efficiencies and selectivities of chiral *N*-triflylphosphoramide catalyzed (3 + 2) cycloaddition between hydrazones and alkenes have been studied through DFT calculations. The acidic *N*-triflylphosphoramide protonates the hydrazone, and a hydrazonium−phosphoramide anion complex is formed. The ion-pair complex is very reactive in the subsequent (3^+ + 2) cycloaddition with alkenes, generating the pyrazolidine product. The alternative 1,3-dipolar (3 + 2) cycloaddition pathway with azomethine imine is less favorable because of the endergonic isomerization from hydrazone to azomethine imine. The Brønsted acid catalyzed (3 + 2) cycloaddition with hydrazone is essentially a (3^+ + 2) cycloaddition with hydrazonium; thus the protonation of hydrazone by the Brønsted acid is crucial for the catalytic efficiency. The less acidic phosphoric acid does not protonate the hydrazone, and a hydrogen-bonded complex is formed. This leads to a large distortion for the hydrogen-bonded complex to achieve the "ion-pair" geometry in the (3 + 2) cycloaddition transition state, resulting in a significant reaction barrier. In addition, we have explained the origins of enantioselectivities when the chiral bulky *N*-triflylphosphoramide is employed. The sterically demanding substituents of phosphoramide catalyst can differentiate the stabilities of the conformers of hydrazone−chiral phosphoramide complex. The most favorable conformer only has one face of the hydrazonium available for alkene approach, which transfers the chirality of the catalyst to the (3^+ + 2) cycloaddition transition state, generating the high enantioselectivity.

ASSOCIATED CONTENT

Supporting Information

Experimental results with more functionalized thioethers, experimental procedures and full characterization of the products and spectra, structures and energies of less favorable regio- and diastereoisomers of selected intermediates and transition states, and coordinates and energies of DFT-computed stationary points. This material is available free of charge via the Internet at http://pubs.acs.org.

AUTHOR INFORMATION

Corresponding Authors

magnus.rueping@rwth-aachen.de
houk@chem.ucla.edu

Author Contributions

‖X.H. and H.B.K. contributed equally.

Notes

The authors declare no competing financial interest.

ACKNOWLEDGMENTS

We are grateful to the National Science Foundation (Grant CHE-1361104) for financial support of this research. M.R. acknowledges the DFG for financial support. We gratefully acknowledge Dr. Vilas B. Phapale for his assistance for the preparation of the catalysts. Dr. M. S. Maji would like to thank the Alexander von Humboldt foundation for the financial support, and Dr. H. B. Kücük thanks the Council of Higher Education of Turkey for a fellowship. We thank Dr. Yong Liang for helpful discussions and Iuliana Atodisresei for help in manuscript preparation. Calculations were performed on the Hoffman2 Cluster at UCLA and the Extreme Science and Engineering Discovery Environment (XSEDE), which is supported by the NSF (Grant OCI-1053575).

REFERENCES

(1) Behr, L. C.; Fusco, R.; Jarboe, C. H. In *Pyrazoles, Pyrazolines, Pyrazolidines, Indazoles and Condensed Rings*; Wiley, R. H., Ed.; The Chemistry of Heterocyclic Compounds, Vol. *22*; Interscience Publishers: New York, 1967.

(2) (a) Gürspy, A.; Demirayak, S.; Capan, G.; Erol, K.; Vural, K. *Eur. J. Med. Chem.* **2000**, *35*, 359. (b) Brzozowski, Z.; Saczewski, F.; Gdaniec, M. *Eur. J. Med. Chem.* **2000**, *35*, 1053. (c) Jeong, T.-S.; Kim, K. S.; An, S.-J.; Cho, K.-H.; Lee, S.; Lee, W. S. *Bioorg. Med. Chem. Lett.* **2004**, *14*, 2715. (d) Camacho, M. E.; Leon, J.; Entrena, A.; Velasco, G.; Carrion, M. D.; Escames, G.; Vivo, A.; Acuna-Castroviejo, D.; Gallo, M. A.; Espinosa, A. *J. Med. Chem.* **2004**, *47*, 5641. (e) Prasad, Y. J.; Rao, A. L.; Prasoona, L.; Murali, K.; Kumar, P. R. *Bioorg. Med. Chem. Lett.* **2005**, *15*, 5030. (f) Goodell, J. R.; Puig-Basagoiti, F.; Forshey, B. M.; Shi, P.-Y.; Ferguson, D. M. *J. Med. Chem.* **2006**, *49*, 2127. (g) Özdemir, Z.; Kandilci, H. B.; Gumusel, B.; Calis, U.; Bilgin, A. A. *Eur. J. Med. Chem.* **2007**, *42*, 373. (h) Özdemir, A.; Turan-Zitouni, G.; Kaplancıkli, Z. A.; Revial, G.; Guven, K. *Eur. J. Med. Chem.* **2007**, *42*, 403. (i) Zhang, X.; Li, X.; Allan, G. F.; Sbriscia, T.; Linton, O.; Lundeen, S. G.; Sui, Z. *J. Med. Chem.* **2007**, *50*, 3857.

(3) (a) Gao, X. C.; Cao, H.; Zhang, L. Q.; Zhang, B. W.; Cao, Y.; Huang, C. H. *J. Mater. Chem.* **1999**, *9*, 1077. (b) Fu, H. B.; Yao, J. N. *J. Am. Chem. Soc.* **2001**, *123*, 1434. (c) Oh, S. W.; Zhang, D. R.; Kang, Y. S. *Mater. Sci. Eng., C* **2004**, *24*, 131.

(4) For recent reviews on 1,3-dipolar cycloadditions, see: (a) Pellissier, H. *Tetrahedron* **2007**, *63*, 3235. (b) Nair, V.; Suja, T. D. *Tetrahedron* **2007**, *63*, 12247. (c) Zhang, W. *Chem. Lett.* **2013**, *42*, 676. For thermal (3 + 2) cycloadditions, see: (d) Grigg, R.; Kemp, J.; Thompson, N. *Tetrahedron Lett.* **1978**, *19*, 2827. (e) Le Fevre, G.; Hamelin, J. *Tetrahedron Lett.* **1979**, *20*, 1757. (f) Snider, B. B.; Conn, R. S. E.; Sealfon, S. *J. Org. Chem.* **1979**, *44*, 218. (g) Grigg, R.; Dowling, M.; Jordan, M. W.; Sridharan, V. *Tetrahedron* **1987**, *43*, 5873. (h) Khau, V. V.; Martinelli, M. J. *Tetrahedron Lett.* **1996**, *37*, 4323.

(5) For Lewis acid catalyzed (3 + 2) cycloadditions with hydrazones, see: (a) Kobayashi, S.; Shimizu, H.; Yamashita, Y.; Ishitani, H.; Kobayashi, J. *J. Am. Chem. Soc.* **2002**, *124*, 13678. (b) Kobayashi, S.; Hirabayashi, R.; Shimizu, H.; Ishitani, H.; Yamashita, Y. *Tetrahedron Lett.* **2003**, *44*, 3351. (c) Yamashita, Y.; Kobayashi, S. *J. Am. Chem. Soc.* **2004**, *126*, 11279. (d) Shirakawa, S.; Lombardi, P. J.; Leighton, J. L. *J. Am. Chem. Soc.* **2005**, *127*, 9974. (e) Frank, E.; Mucsi, Z.; Zupko, I.; Rethy, B.; Falkay, G.; Schneider, G.; Wölfling, J. *J. Am. Chem. Soc.* **2009**, *131*, 3894. (f) Zamfir, A.; Schenker, S.; Bauer, W.; Clark, T.; Tsogoeva, S. B. *Eur. J. Org. Chem.* **2011**, 3706. (g) Xie, H.; Zhu, J.; Chen, Z.; Li, S.; Wu, Y. *Synthesis* **2011**, 2767.

(6) For recent catalytic asymmetric syntheses of pyrazolines and pyrazolidines, see: (a) LaLonde, R. L.; Wang, Z. J.; Mba, M.; Lackner, A. D.; Toste, F. D. *Angew. Chem., Int. Ed.* **2010**, *49*, 598. (b) Hashimoto, T.; Maeda, Y.; Omote, M.; Nakatsu, H.; Maruoka, K. *J. Am. Chem. Soc.* **2010**, *132*, 4076. (c) Zamfir, A.; Tsogoeva, S. B.

Synthesis **2011**, 1988. (d) Hashimoto, T.; Omote, M.; Maruoka, K. *Angew. Chem., Int. Ed.* **2011**, *50*, 3489. (e) Fernández, M.; Reyes, E.; Vicario, J. L.; Badía, D.; Carrillo, L. *Adv. Synth. Catal.* **2012**, *354*, 371. (f) Hashimoto, T.; Kimura, H.; Kawamata, Y.; Maruoka, K. *Nat. Chem.* **2011**, *3*, 642. (g) Deiana, L.; Zhao, G.-L.; Leijonmarck, H.; Sun, J.; Lehmann, C. W.; Córdova, A. *ChemistryOpen* **2012**, *1*, 134. (h) Müller, S.; List, B. *Angew. Chem., Int. Ed.* **2009**, *48*, 9975.

(7) Rueping, M.; Maji, M. S.; Küçük, H. B.; Atodiresei, I. *Angew. Chem., Int. Ed.* **2012**, *51*, 12864.

(8) For related work in the field of chiral BINOL-based *N*-triflylphosphoramides, see: (a) Yamamoto, S. A.; Nakashima, D.; Yamamoto, H. *J. Am. Chem. Soc.* **2006**, *128*, 9626. For an overview, see: (b) Rueping, M.; Nachtsheim, B. J.; Ieawsuwan, W.; Atodiresei, I. *Angew. Chem., Int. Ed.* **2011**, *50*, 6706. For further examples, see: (c) Rueping, M.; Ieawsuwan, W.; Antonchick, A. P.; Nachtsheim, B. J. *Angew. Chem., Int. Ed.* **2007**, *46*, 2097. (d) Rueping, M.; Nachtsheim, B. J.; Moreth, S. A.; Bolte, M. *Angew. Chem., Int. Ed.* **2008**, *47*, 593. (e) Rueping, M.; Theissmann, T.; Kuenkel, A.; Koenigs, R. M. *Angew. Chem., Int. Ed.* **2008**, *47*, 6798. (f) Enders, D.; Narine, A. A.; Toulgoat, F.; Bisschops, T. *Angew. Chem., Int. Ed.* **2008**, *47*, 5661. (g) Zeng, M.; Kang, Q.; He, Q.-L.; You, S.-L. *Adv. Synth. Catal.* **2008**, *350*, 2169. (h) Rueping, M.; Ieawsuwan, W. *Adv. Synth. Catal.* **2009**, *351*, 78. (i) Rueping, M.; Nachtsheim, B. J.; Koenigs, R. M.; Ieawsuwan, W. *Chem.—Eur. J.* **2010**, *16*, 13116. (j) Rueping, M.; Lin, M.-Y. *Chem.—Eur. J.* **2010**, *16*, 4169. (k) Rueping, M.; Nachtsheim, B. J. *Synlett* **2010**, 119. (l) Rueping, M.; Merino, E.; Koenigs, R. M. *Adv. Synth. Catal.* **2010**, *352*, 2629. (m) Cheon, C. H.; Yamamoto, H. *Org. Lett.* **2010**, *12*, 2476. (n) Rueping, M.; Uria, U.; Lin, M.-Y.; Atodiresei, I. *J. Am. Chem. Soc.* **2011**, *133*, 3732. (o) Hashimoto, T.; Nakatsu, H.; Yamamoto, K.; Maruoka, K. *J. Am. Chem. Soc.* **2011**, *133*, 9730. (p) Rueping, M.; Ieawsuwan, W. *Chem. Commun.* **2011**, *47*, 11450.

(9) For SPINOL-derived phosphoric acid catalysts, see: (a) Jia, Y.-X.; Zhong, J.; Zhu, S.-F.; Zhang, C.-M.; Zhou, Q.-L. *Angew. Chem., Int. Ed.* **2007**, *46*, 5565. (b) Xie, J.-H.; Zhou, Q.-L. *Acc. Chem. Res.* **2008**, *41*, 581. (c) Coric, I.; Muller, S.; List, B. *J. Am. Chem. Soc.* **2010**, *132*, 17370. (d) Xing, C.-H.; Liao, Y.-X.; Ng, J.; Hu, Q.-S. *J. Org. Chem.* **2011**, *76*, 4125. (e) Xu, B.; Zhu, S.-F.; Xie, X.-L.; Shen, J.-J.; Zhou, Q.-L. *Angew. Chem., Int. Ed.* **2011**, *50*, 11483. (f) Xing, C.-H.; Liao, Y.-X.; Ng, J.; Hu, Q.-S. *J. Org. Chem.* **2011**, *76*, 4125. (g) Huang, D.; Xu, F.; Lin, X.; Wang, Y. *Chem.—Eur. J.* **2012**, *18*, 3148. (h) Huang, D.; Xu, F.; Chen, T.; Wang, Y.; Lin, X. *RSC Adv.* **2013**, *3*, 573. (i) Zhao, Y.; Li, X.; Mo, F.; Li, L.; Lin, X. *RSC Adv.* **2013**, *3*, 11895. (j) Huang, D.; Li, X.; Xu, F.; Li, L.; Lin, X. *ACS Catal.* **2013**, *3*, 2244. (k) Xu, B.; Zhu, S.-F.; Zhang, Z.-C.; Yu, Z.-X.; Ma, Y.; Zhou, Q.-L. *Chem. Sci.* **2014**, *5*, 1442. (l) Wang, S.-G.; You, S.-L. *Angew. Chem., Int. Ed.* **2014**, *53*, 2194. (m) Xu, B.; Zhu, S.-F.; Zuo, X.-D.; Zhang, Z.-C.; Zhou, Q.-L. *Angew. Chem., Int. Ed.* **2014**, *53*, 3913.

(10) Kaupmees, K.; Tolstoluzhsky, N.; Raja, S.; Rueping, M.; Leito, I. *Angew. Chem., Int. Ed.* **2013**, *51*, 11569.

(11) (a) Domingo, L. R. *Eur. J. Org. Chem.* **2000**, 2265. (b) Tanaka, J.; Kanemasa, S. *Tetrahedron* **2001**, *57*, 899. (c) Wagner, G. *Chem.—Eur. J.* **2003**, *9*, 1503. (d) Kuznetsov, M. L.; Kukushkin, V. Y.; Haukka, M.; Pombeiro, A. J. L. *Inorg. Chim. Acta* **2003**, *356*, 85. (e) Castillo, R.; Andrés, J.; Domingo, L. R. *Eur. J. Org. Chem.* **2005**, 4705. (f) Domingo, L. R.; Benchouk, W.; Mekelleche, S. M. *Tetrahedron* **2007**, *63*, 4464. (g) Wagner, G.; Danks, T. N.; Vullo, V. *Tetrahedron* **2007**, *63*, 5251. (h) Bădoiu, A.; Bernardinelli, G.; Mareda, J.; Kündig, E. P.; Viton, F. *Chem.—Asian J.* **2008**, *3*, 1298. (i) Wagner, G.; Danks, T. N.; Desai, B. *Tetrahedron* **2008**, *64*, 477. (j) Frank, É.; Mucsi, Z.; Szécsi, M.; Zupkó, I.; Wölfling, J.; Schneider, G. *New J. Chem.* **2010**, *34*, 2671. (k) Chaudhuri, T.; Banerjee, M. J. *Luminescence* **2012**, *132*, 1456. (l) Śnieżek, M.; Stecko, S.; Panfil, I.; Furman, B.; Urbańczyk-Lipkowska, Z.; Chmielewski, M. *Tetrahedron: Asymmetry* **2013**, *24*, 89.

(12) (a) Hesse, K.-D. *Justus Liebigs Ann. Chem.* **1970**, *743*, 50. (b) Le Fevre, G.; Sinbandhit, S.; Hamelin, J. *Tetrahedron* **1979**, *35*, 1821. (c) Wilson, R. M.; Rekers, J. W. *J. Am. Chem. Soc.* **1979**, *101*, 4005. (d) Fouchet, B.; Joucla, M.; Hamelin, J. *Tetrahedron Lett.* **1981**, *22*, 1333. (e) Shimizu, T.; Hayashi, Y.; Nakano, M.; Teramura, K. *Bull. Chem. Soc. Jpn.* **1982**, *55*, 2456. (f) Shimizu, T.; Hayashi, Y.; Teramura, K. *Bull. Chem. Soc. Jpn.* **1985**, *58*, 397. (g) Shimizu, T.; Hayashi, Y. Y.; Miki, M.; Teramura, K. *J. Org. Chem.* **1987**, *52*, 2277. (h) Griffith, A. K.; Vanos, C. M.; Lambert, T. H. *J. Am. Chem. Soc.* **2012**, *134*, 18581. (i) Davis, L. O.; Daniel, W. F. M.; Tobey, S. L. *Tetrahedron Lett.* **2012**, *53*, 522. (j) Lin, G.-Q.; Lei, X.; Liu, P.; Xu, Q.-Q.; Dong, C. *Synlett* **2012**, *23*, 2087.

(13) The absolute configuration at the C3 stereocenter was assigned in analogy to our previously reported compounds.[7]

(14) Detailed experimental results with other thioethers are included in Supporting Information.

(15) The reaction tolerates various alkyl substituents on vinyl ethers with moderate to high enantioselectivities, and the ethyl vinyl ether gives the highest yield:

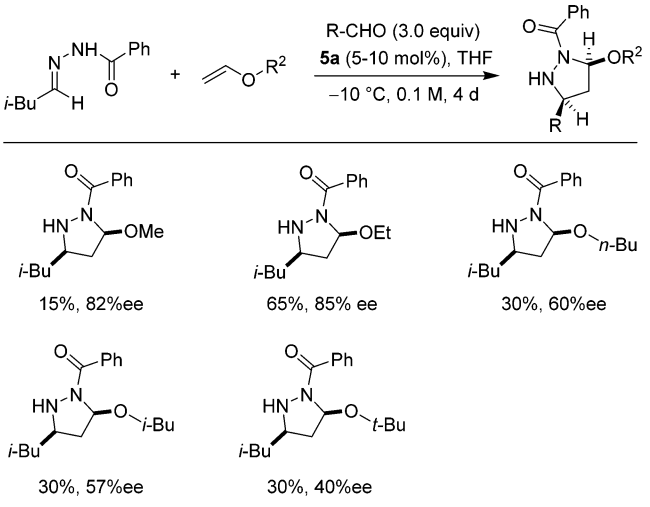

Also, the reaction with 2,3-dihydrofuran gives racemic products, and the reaction with 3,4-dihydro-2*H*-pyran does not produce the desired cycloadduct.

(16) The reactions with enamides only give racemic products or no desired cycloadducts:

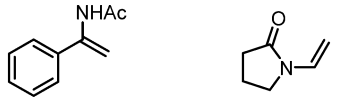

(17) Frisch, M. J.; Trucks, G. W.; Schlegel, H. B.; Scuseria, G. E.; Robb, M. A.; Cheeseman, J. R.; Scalmani, G.; Barone, V.; Mennucci, B.; Petersson, G. A.; Nakatsuji, H.; Caricato, M.; Li, X.; Hratchian, H. P.; Izmaylov, A. F.; Bloino, J.; Zheng, G.; Sonnenberg, J. L.; Hada, M.; Ehara, M.; Toyota, K.; Fukuda, R.; Hasegawa, J.; Ishida, M.; Nakajima, T.; Honda, Y.; Kitao, O.; Nakai, H.; Vreven, T.; Montgomery, J. A., Jr.; Peralta, J. E.; Ogliaro, F.; Bearpark, M.; Heyd, J. J.; Brothers, E.; Kudin, K. N.; Staroverov, V. N.; Kobayashi, R.; Normand, J.; Raghavachari, K.; Rendell, A.; Burant, J. C.; Iyengar, S. S.; Tomasi, J.; Cossi, M.; Rega, N.; Millam, J. M.; Klene, M.; Knox, J. E.; Cross, J. B.; Bakken, V.; Adamo, C.; Jaramillo, J.; Gomperts, R.; Stratmann, R. E.; Yazyev, O.; Austin, A. J.; Cammi, R.; Pomelli, C.; Ochterski, J. W.; Martin, R. L.; Morokuma, K.; Zakrzewski, V. G.; Voth, G. A.; Salvador, P.; Dannenberg, J. J.; Dapprich, S.; Daniels, A. D.; Farkas, O.; Foresman, J. B.; Ortiz, J. V.; Cioslowski, J.; Fox, D. J. *Gaussian 09*, revision D.01; Gaussian, Inc.: Wallingford, CT, 2009.

(18) (a) Zhao, Y.; Truhlar, D. *Theor. Chem. Acc.* **2008**, *120*, 215. (b) Zhao, Y.; Truhlar, D. G. *Acc. Chem. Res.* **2008**, *41*, 157.

(19) (a) Barone, V.; Cossi, M. *J. Phys. Chem. A* **1998**, *102*, 1995. (b) Cossi, M.; Rega, N.; Scalmani, G.; Barone, V. *J. Comput. Chem.* **2003**, *24*, 669. (c) Takano, Y.; Houk, K. N. *J. Chem. Theory Comput.* **2005**, *1*, 70.

(20) There is an unfavorable regio-isomer for each complex in Figure 1; the structures and relative Gibbs free energies are shown in Supporting Information.

(21) The double hydrogen-bond formations are only possible in complex **16** and its less stable regio-isomer.
(22) We find that the barrier of (3 + 2) cycloaddition between hydrazone and ethylene (without the hydrogen-bonded phosphoramide) is 47.4 kcal/mol, 3.9 kcal/mol lower than the barrier with the hydrogen-bonded complex **16**.
(23) The (3 + 2) cycloaddition barrier between hydrazonium cation and ethylene is 26.0 kcal/mol. For related computational study on the (3 + 2) cycloaddition with hydrazonium cation, see: Hong, X.; Liang, Y.; Griffith, A. K.; Lambert, T. H.; Houk, K. N. *Chem. Sci.* **2014**, *5*, 471.
(24) The structures and energies of less stable transition states that lead to the diastereomers are shown in Supporting Information.
(25) In experiment, more reactive cyclopentadiene and styrene derivatives are used, and the calculated cycloaddition barrier between complex **13** and α-methylstyrene is 23.5 kcal/mol, which is consistent with the experimental conditions (RT, 18 h).
(26) (a) Ess, D. H.; Houk, K. N. *J. Am. Chem. Soc.* **2007**, *129*, 10646. (b) Ess, D. H.; Houk, K. N. *J. Am. Chem. Soc.* **2008**, *130*, 10187.
(27) For reviews, see: (a) van Zeist, W.-J.; Bickelhaupt, F. M. *Org. Biomol. Chem.* **2010**, *8*, 3118. (b) Fernández, I. *Phys. Chem. Chem. Phys.* **2014**, *16*, 7662. (c) Fernández, I.; Bickelhaupt, F. M. *Chem. Soc. Rev.* **2014**, *43*, 4953.
(28) For selected recent examples, see: (a) Gordon, C. G.; Mackey, J. L.; Jewett, J. C.; Sletten, E. M.; Houk, K. N.; Bertozzi, C. R. *J. Am. Chem. Soc.* **2012**, *134*, 9199. (b) Liang, Y.; Mackey, J. L.; Lopez, S. A.; Liu, F.; Houk, K. N. *J. Am. Chem. Soc.* **2012**, *134*, 17904. (c) Lopez, S. A.; Houk, K. N. *J. Org. Chem.* **2013**, *78*, 1778. (d) Fernández, I.; Sola, M.; Bickelhaupt, F. M. *Chem.—Eur. J.* **2013**, *19*, 7416. (e) Kamber, D. N.; Nazarova, L. A.; Liang, Y.; Lopez, S. A.; Patterson, D. M.; Shih, H.-W.; Houk, K. N.; Prescher, J. A. *J. Am. Chem. Soc.* **2013**, *135*, 13680. (f) Liu, F.; Paton, R. S.; Kim, S.; Liang, Y.; Houk, K. N. *J. Am. Chem. Soc.* **2013**, *135*, 15642. (g) Morin, M. S. T.; St-Cyr, D. J.; Arndtsen, B. A.; Krenske, E. H.; Houk, K. N. *J. Am. Chem. Soc.* **2013**, *135*, 17349. (h) Yang, J.; Liang, Y.; Seckute, J.; Houk, K. N.; Devaraj, N. K. *Chem.—Eur. J.* **2014**, *20*, 3365. (i) Fernández, I.; Bickelhaupt, F. M. *J. Comput. Chem.* **2014**, *35*, 371. (j) Liu, S.; Lei, Y.; Qi, X.; Lan, Y. *J. Phys. Chem. A* **2014**, *118*, 2638. (k) Cao, Y.; Liang, Y.; Zhang, L.; Osuna, S.; Hoyt, A.-L. M.; Briseno, A. L.; Houk, K. N. *J. Am. Chem. Soc.* **2014**, *136*, 10743. (l) Liu, F.; Liang, Y.; Houk, K. N. *J. Am. Chem. Soc.* **2014**, *136*, 11483. (m) Hong, X.; Liang, Y.; Brewer, M.; Houk, K. N. *Org. Lett.* **2014**, *16*, 4260.
(29) For related computational studies on the chiral phosphoric acid catalysts, see: (a) Marcelli, T.; Hammar, P.; Himo, F. *Chem.—Eur. J.* **2008**, *14*, 8562. (b) Simón, L.; Goodman, J. M. *J. Am. Chem. Soc.* **2008**, *130*, 8741. (c) Marcelli, T.; Hammar, P.; Himo, F. *Adv. Synth. Catal.* **2009**, *351*, 525. (d) Simón, L.; Goodman, J. M. *J. Am. Chem. Soc.* **2009**, *131*, 4070. (e) Simón, L.; Goodman, J. M. *J. Org. Chem.* **2010**, *75*, 589. (f) Simón, L.; Goodman, J. M. *J. Org. Chem.* **2011**, *76*, 1775. (g) Grayson, M. N.; Pellegrinet, S. C.; Goodman, J. M. *J. Am. Chem. Soc.* **2012**, *134*, 2716. (h) Wang, H.; Jain, P.; Antilla, J. C.; Houk, K. N. *J. Org. Chem.* **2013**, *78*, 1208. (i) Grayson, M. N.; Goodman, J. M. *J. Am. Chem. Soc.* **2013**, *135*, 6142. (j) Maity, P.; Pemberton, R. P.; Tantillo, D. J.; Tambar, U. K. *J. Am. Chem. Soc.* **2013**, *135*, 16380. (k) Calleja, J.; González-Pélez, A. B.; de Lera, Á. R.; Álvarez, R.; Fañanás, F. J.; Rodriguez, F. *Chem. Sci.* **2014**, *5*, 996. (l) Meng, S.-S.; Liang, Y.; Cao, K.-S.; Zou, L.; Lin, X.-B.; Yang, H.; Houk, K. N.; Zheng, W.-H. *J. Am. Chem. Soc.* **2014**, *136*, 12249.
(30) Qualitative description of the size of binding pockets of [H8]-BINOL-based and SPINOL-based *N*-triflylphosphoramide catalysts:

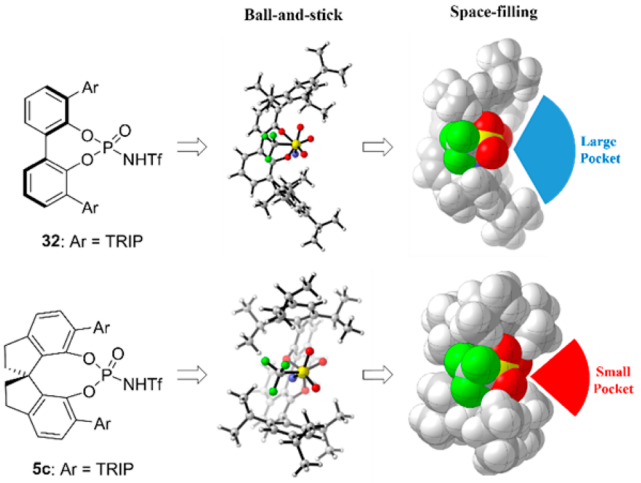

dx.doi.org/10.1021/ja506660c | *J. Am. Chem. Soc.* 2014, 136, 13769−13780